

CONSIDERATION OF POSSIBLE INDICATORS FOR WHIPLASH INJURY ASSESSMENT AND EXAMINATION OF SEAT DESIGN PARAMETERS USING HUMAN FE MODEL

Yuichi Kitagawa

Tsuyoshi Yasuki

Junji Hasegawa

Toyota Motor Corporation

Japan

Paper Number 07-0093

ABSTRACT

Rear impact simulations were conducted using a validated human body FE model representing an average-sized male occupant. Prototype seat models were also prepared to simulate actual rear impact conditions. The features of occupant responses including head and neck kinematics were investigated considering the interaction between the occupant and the seat (and the head restraint). NIC and joint capsule strain (JCS) were taken as injury indicators. NIC is a widely used indicator in laboratory tests, while the joint capsules have recently been focused on as a potential site of neck pain. Precise modeling of the neck soft tissues enabled the estimation of tissue level injury. The results suggested that NIC corresponds to the difference in motion between the head and the torso, while JCS indicates the difference in their position. Two studies on seat design changes were conducted to examine the contribution from the seat design parameters and to understand the meaning of injury indicators. A parametric study was conducted on thirteen cases where major seat design factors were changed on a single seat configuration, while the second study focused on three different seat configurations with greater differences in dimensions, structure, and mechanical and material properties. The parametric study revealed that the stiffness of the reclining joint greatly affects the resultant NIC values, while JCS was more influenced by the thickness of the upper-end of the seat-back frame. The other finding showed strong correlations between NIC and the head restraint contact timing (HRCT), and JCS and the neck leaning angle (NLA). Introducing the results of the three different seat configurations, the second study suggests that NLA could be used as an injury indicator instead of JCS in dummy tests, while HRCT would not be a good indicator in terms of injury assessment.

INTRODUCTION

It is generally understood that rear-end collisions and associated neck injuries are relatively common in traffic accidents in many countries. In Japan, the number of rear-end collisions has increased during

this decade even while the number of fatalities has decreased, based on a report from the Japanese National Police Agency [1]. A typical neck injury form is known as 'whiplash' which is not life-threatening but is accompanied by dull pain that is sometimes long lasting. Despite the frequency of rear-end collisions and whiplash injuries, its injury mechanism is not completely understood. Because whiplash injuries are relatively minor and are not necessarily accompanied by obvious clinically detectable tissue damage, it is not easy to identify the relationship between loading to the neck and injury outcome. A common understanding is that relative motion between the head and the torso may load the neck in a way not generated in natural (physiological) motions. Hyperextension of the neck was thought to be a cause of injury based on this aspect. However, it was recognized as not being a significant factor considering the fact that whiplash injuries were still reported even after most vehicles were equipped with head restraints. In order to understand a possible injury mechanism without causing large neck extension, cervical kinematics have been studied with human subjects (Deng et al. [2], Ono et al. [3]). Svensson et al. [4] aimed at a form of neck retraction where the head stays at the same place but the torso is pushed forward, resulting in the cervical spine causing an s-shape. Bostrom et al. [5] proposed an injury indicator called NIC assuming that the pressure gradient in the spinal fluid generated in the s-shape motion could be a cause of injury. Regardless of the controversy related to injury mechanisms, NIC has become a popular indicator because it actually includes relative acceleration and velocity terms between the head and the torso in its formulation. Recent studies focus more on facet joint motions, as the whole of cervical kinematics is related to a series of vertebral motions and motion is generated along or around the facet joints. Based on a hypothesis that the facet joint capsules could be a potential site of neck pain, deformation of the capsule tissue has been analyzed sometimes in a functional spine unit (Winkelstein et al. [6]) and sometimes in a whole body (Sundararajan et al. [7]). Lu et al. [8] studied the neural response of the facet joint capsules under stretch applying artificial stimulation to animal subjects. These results suggested a possible

mechanism of neck pain that supports the hypothesized role of joint capsule strain in whiplash injury. The objective of this study is to analyze cervical kinematics based on finite element analysis simulating rear impacts, taking into account the hypothesis mentioned above, and then to discuss the validity of possible indicators for whiplash injury assessment. The study also examines the influence of seat design parameters on the injury indicators.

METHODS

Human Body Modeling

A finite element human body model named the Total Human Model for Safety (THUMS) is used in this study. The model was developed in collaboration between Toyota Motor Corporation and Toyota Central Research and Development Laboratory. The skeletal system of the human body including joints was precisely modeled to simulate occupant/pedestrian behavior in car crashes. The cortical part of bones was modeled with shell elements while the trabecular part was modeled with solid elements. The geometry (feature lines) of each bony part was based on a commercial human body database ViewPoint™, but the finite element mesh was newly generated. The ligaments connecting bony parts were also included in the model. The length, thickness and insertion points of the ligaments were carefully defined referring to anatomy textbooks. Soft tissues surrounding the bones such as skin, fat and muscles were represented by a single solid layer. The muscles along the cervical spine were separately modeled with 1D elements to simulate passive muscular responses under stretch by external forces. The brain and internal organs were also included but simplified as solid blocks. Material properties for these parts were defined referring to the literature [9], [10]. The entire model has 60,000 nodes and 80,000 elements with a time-step of approximately one microsecond in an explicit time integration scheme. The body size represents a 50th percentile adult male (AM50) with a height of 175 cm and weighing 77 kg. The model runs on a commercial finite element software LS-DYNA™. Basically, the model (Version 1.61) has been validated against literature data where Post Mortem Human Subject (PMHS) were impacted at different body parts at various loading conditions [11], [12]. In this study, the neck part of the model was revised to further examine cervical kinematics in rear impacts. Figure 1 shows the anatomy of the cervical vertebrae and models. As described above, the ligaments in the joints were modeled so as to connect adjacent vertebrae. The major ligaments are the anterior longitudinal ligament (ALL), the posterior longitudinal ligament (PLL), the ligamentum flavum (LF), the interspinous ligament (ITL), the supraspinous ligaments (SSL), and the

intertransverse ligament (ISL). Relative motion between adjacent vertebrae generally occurs around the facet joints located on the right and left sides of the neural arch. The joints are covered with the joint capsules. The capsule tissues were modeled with membrane elements. The joints can move along or around the facet joint surfaces with some resistance and under some restriction from the ligaments.

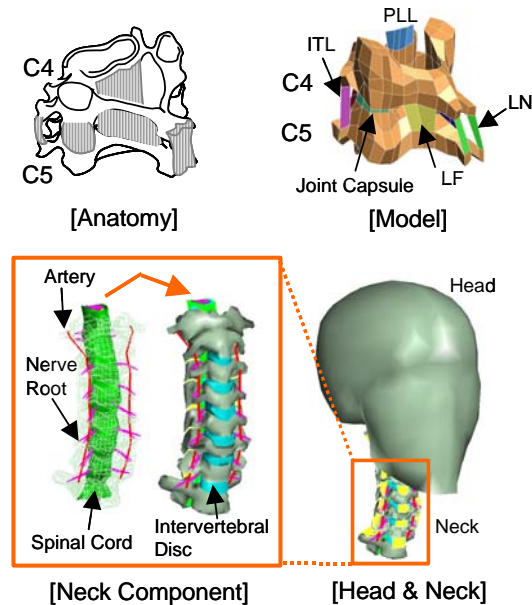


Figure 1. Anatomy of Cervical Vertebrae and Models.

Model Validation

The model has been previously validated against literature data by the authors [13]. The validation was conducted at three levels: component level, subsystem level and whole body level. Only the validation at component level was described in this paper. Siegmund et al. [14] conducted a series of PMHS tests where the unit of C3-C4 was subjected to shear loading with compressive force as shown in Figure 2. Anterior-posterior (A-P) displacement and sagittal rotation of C3 with respect to C4 were measured in the tests. Additionally, the maximum principal strain in the joint capsule was estimated by measuring distance change among markers posted to the tissue. The corresponding part of the C3-C4 unit was extracted from the THUMS neck model, and then equivalent boundary conditions were applied to the model. The A-P displacement of C3 was obtained directly from nodal output while the sagittal rotation was calculated from nodal displacement data of two vertebrae. The maximum principal strain in the joint capsule was directly output from the elements forming that part. Figure 3 compares the measured and calculated data. A-P displacement, sagittal rotation and joint capsule strain were plotted with respect to the applied shear force. Corridors were created connecting upper points and lower points in

the measured data while the calculated results were plotted as curves. The calculated curve for the A-P displacement and that for the sagittal rotation are within the range of the corridors. It was found that the calculated A-P displacement and sagittal rotation were within the test corridors. On the other hand, the calculated joint capsule strain did not have a good match with the test data. The strain rose rapidly at the beginning then showed a flat corridor in the test data while it increased linearly in the model. The cause of the initial rise in the test corridor is not clear while the reason for the latter difference may be an assumption in modeling. In the THUMS neck model, the joint capsule elements simply connect the nodes at the edges of joint surfaces while the actual joint capsules cover a wider area surrounding the joint surfaces. The length of the capsule elements is around 1.2 mm which is around 20% of the actual tissue. This difference may lead overestimating the strain level in the model. Due to the imprecision in modeling the capsule tissue and in predicting absolute strain values, only relative evaluations comparing cases were conducted in this study. Seat models are necessary to conduct rear impact simulations. Three prototype seats with different configurations (dimensions, structures and materials) were modeled for the study. In each model, the geometrical features, construction of components, and mechanical and material properties of the components were carefully incorporated. Figure 4 shows overall views of the seat models. The models were then validated against test data as assembled seat systems. Considering a typical loading case in rear impacts where the occupant loads on the seat-back, the mechanical responses of the actual prototype seats were examined applying quasi-static loading to the upper end of the seat-back frames. Simulations were conducted on the models to duplicate the loading tests. The moment around the reclining joint and the rotational angle of the seat-back were compared between the test data and the simulation results to confirm the validity of the model. Figure 5 shows an example of validation on Seat A. A linear increasing trend in the calculated data showed a good match with the test data.

Rear Impact Simulation

A rear impact simulation was conducted using the Seat A model with THUMS in a seated position. The posture of THUMS was adjusted to a standard seating position supposing an AM50 size front-seat occupant. The hip point (including the torso angle) was adjusted first. Then the femur angle was given considering the height difference from the floor-pan. During the adjusting process, deformation of the seat cushion was considered for the initial geometry. The seat was mounted on a rigid plate representing a floor-pan. Contacts were defined between the torso back and the seat-back, the head (occiput) and the

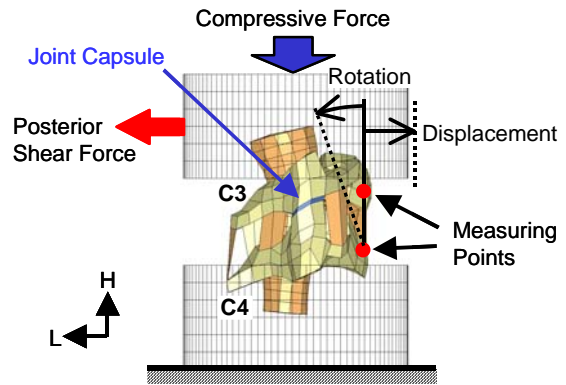


Figure 2. C3-C4 Joint Model for Validation.

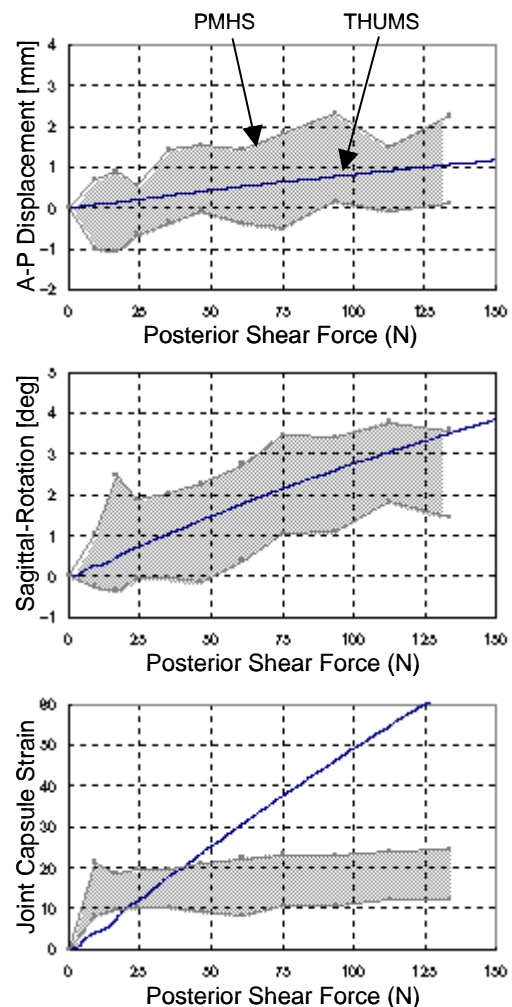


Figure 3. Comparison of A-P Displacement, Sagittal Rotation and Joint Capsule Strain between PMHS and THUMS.

head restraint, the buttocks and the seat pan to handle interaction among them. The impact condition was defined so as to simulate an actual rear impact case. Kraft et al. [15] analyzed acceleration pulses of actual rear collisions obtained from vehicles fitted with data recorders, and have



Figure 4. Prototype Seat Models.

proposed representative pulse curves to be used as acceleration input in sled tests. Research organizations like Folksam, IIWPG and ADAC have adopted these proposed acceleration pulses to help evaluate the performance of production vehicle seats. A triangular pulse with a delta-V of 16 km/h is the most popular impact condition adopted in laboratory tests. A delta-V of 16 represents a rear-end collision where one vehicle strikes another vehicle with the same weight at 32 km/h. According to a study conducted by the Ministry of Land, Infrastructure and Transport of Japan [16], this impact condition is more severe than 60 percent of all rear collisions on the roads in Japan. By elevating the delta-V to 25 km/h, which corresponds to a vehicle to vehicle collision at 50 km/h, approximately 90 percent of all rear collisions are less severe. This study adopted the higher delta-V to understand the cervical kinematics in relatively severe conditions, and to magnify the influence of the seat design parameters. Figure 6 shows a triangular acceleration pulse that is used as an input to accelerate the sled in the forward direction (X-direction). The simulation was terminated 200 ms after impact. Time history data for displacement, velocity and acceleration were output at selected nodes as well as the entire motion in the model. NIC and joint capsule strain (JCS) were then examined. NIC was calculated from the acceleration and velocity data. JCS was represented by the maximum principal strain in the capsule tissue. The strain value was output directly from the elements composing the capsule part. Only the maximum value in the capsule elements among the cervical joints was taken for evaluation.

Seat Design Study

Two studies were conducted to examine the influence of seat design. The first one was a parametric study conducted on a single seat configuration but changing parameters that would potentially affect the head-neck motion of the occupant in a rear impact. The Seat B model was chosen for the study. The selected parameters were; the fore-aft and vertical locations of the head

restraint, the stiffness of the head restraint foam material, the thickness of the seat-back upper-end frame, the stiffness of the reclining joint, and the stiffness of the bracket plate inserted between the seat-pan and the seat adjusting rails. Table 1 summarizes the parameters and the range of design change assumed for each parameter. A total of thirteen cases was prepared based on the Seat B configuration with different specifications. The ranges of design parameters were determined considering possible high and low values that could be seen in actual prototype seats. Rear impact simulations were conducted for the thirteen cases using the same acceleration pulse (Figure 6) for the

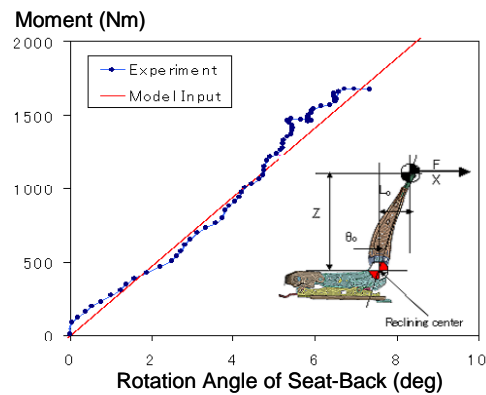


Figure 5. Validation of Mechanical Response of Reclining Joint in Seat A.

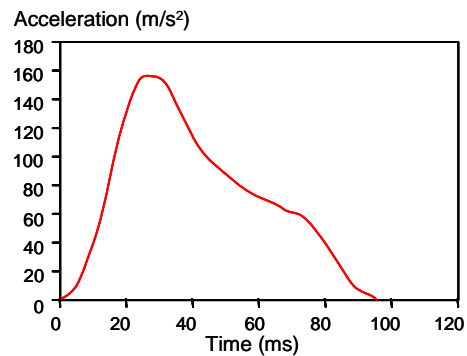


Figure 6. Triangle Acceleration Pulse for Input.

input. Instead of analyzing time history responses of the occupant head and neck, the results were evaluated with NIC and joint capsule strain to identify a dominant parameter for the indicators. The second study was conducted considering differences in seat configuration. The purpose of this study was to investigate the correlation among the whiplash injury indicators proposed by researchers and adopted in some assessment tests. The examined indicators were NIC and JCS as already used in the previous study, head restraint contact timing (HRCT) and neck leaning angle (NLA). HRCT is the timing when the head contacts the head restraint. This indicator is actually adopted in some assessment tests as a seat design factor but not as an injury indicator. There is discussion if the indicator really reflects the whiplash injury risk in terms of assessment [13]. In rear impact simulations, HRCT can be detected by monitoring the contact force between two parts. NLA is the rotation angle of the head with respect to T1 as shown in Figure 7. The reason for using this indicator is that JCS is only available in FE simulations with a human body model that has cervical joint capsule tissues. It is practical to have an alternative indicator that is measurable on the crash test dummy. All three seat models shown in Figure 4 were used in this study. The geometry and dimensions, composition of mechanical parts, and mechanical and material properties of the components are completely different among the seats. Using the Seat B model as the reference base, the Seat A model has relatively lower stiffness in its reclining joint, less rigidity in its head restraint support and a head restraint located more to the rear with respect to the upper-end frame. The Seat C model has higher stiffness in the reclining joint, more rigidity in the head restraint support, and a head restraint located in the forward direction.

Rear impact simulations were conducted using these seat models in the same manner as described above. The sitting postures of the occupant on these three seat models were the basically the same but were adjusted to those used in seat design. The indicators, NIC, JCS, HRCT, and NLA, were calculated from the results. The correlations among the indicators were investigated in detail.

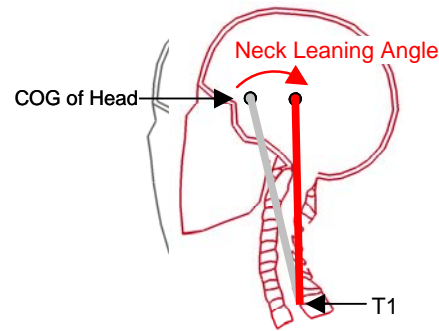


Figure 7. Definition of Neck Leaning Angle.

RESULTS

Results of Rear Impact Simulation

Figure 8 shows the entire motion of THUMS on Seat A observed from a lateral view. The frames were selected considering interaction events between the occupant body and the seat. In the initial seating posture, there is a small gap between the occiput and the head restraint, while the lower torso contacts the seat-back. The torso is pushed forward immediately after the rear impact begins, while the head does not move until the gap becomes zero. In this case, the head contacts the head restraint around 50 ms. The seat-back frame deforms rearward as the occupant body loads on it. The deformation of the seat-back frame reaches its maximum peak around 100 ms. The torso starts moving back forward after this, which is called a 'rebound' motion. The head still moves back for a while but the head restraint deformation reaches its maximum peak before long. It was around 130 ms in this case. Then the head starts moving forward again. Figure 9 shows the acceleration responses at the head, T1, and pelvis. As the buttocks remain in the seat, the pelvis acceleration rises immediately after impact. Although the lower torso also remains against the seat-back, there is some delay in acceleration rise at T1 because of the small gap between the upper torso and the seat-back. The head acceleration does not start until the occupant contacts the head restraint. The

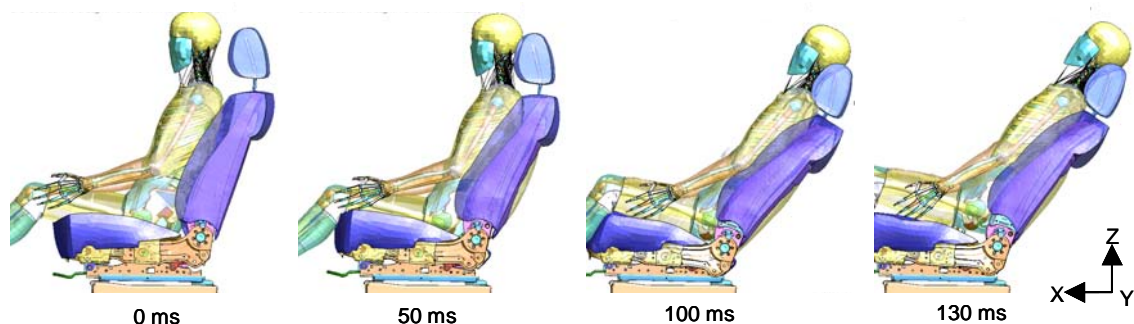


Figure 8. Gross Motion of THUMS Occupant in Rear Impact (Seat A, Delta-V=25km/h).

pelvis and the head show triangular acceleration pulses, while that of T1 has two peaks. The maximum peak in the T1 acceleration is lower than that in the pelvis, while the head acceleration has a higher peak than the pelvis. The convergence of the acceleration pulses occurs in the same order as seen in the rising timings. Contact forces between the occupant body and the seat are plotted in Figure 10. The contact force at the pelvis indicates the force between the buttocks and the seat-back, while the contact force at the torso indicates that between the torso-back and the seat-back, where the boundary between the buttocks and the torso-back is assumed

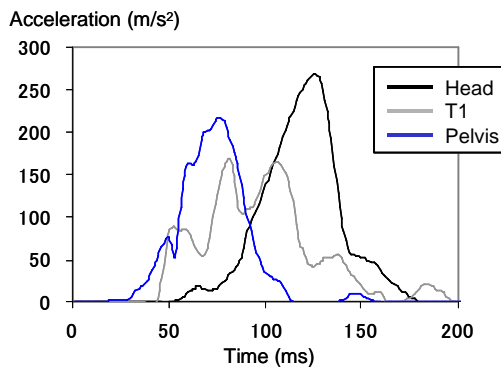


Figure 9. X-accelerations at Head, T1 and Pelvis.

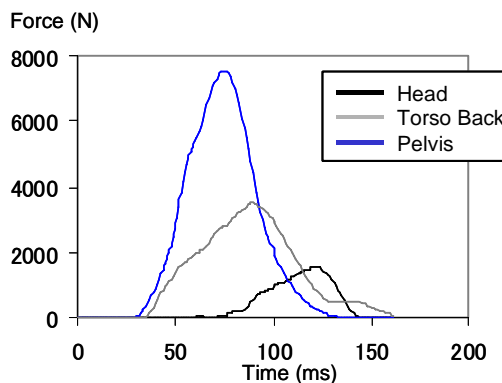


Figure 10. Contact Forces between Head, Tor Back, Pelvis and Seat.

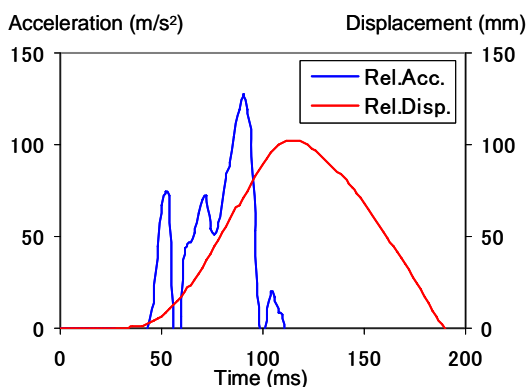


Figure 11. Relative Acceleration and Relative Displacement between Head and T1.

around the waist. The contact force at the head is the force between the occiput and the head restraint. The order of rising timings is exactly the same; the pelvis is first, followed by the thorax and the head is the last. The rising timings are around 30, 40 and 70 ms respectively. The maximum force peak is largest at the pelvis, followed by the thorax and the head. Figure 11 shows the relative acceleration and the relative displacement between the head and T1. Only the positive part of the relative acceleration is shown in this figure, in which the head acceleration is higher than that of the pelvis. The maximum peak around 50 ms indicates the initial peak in relative motion between the head and the torso. This is called 'retraction.' There is another peak around 80 ms with higher amplitude. The relative acceleration finally converges to zero around 100 ms after impact. The displacement data was output from the same nodes where the acceleration values were obtained. There is mostly the positive part up to 200 ms, in which the head is in the posterior side of the torso. There is only one peak in the relative displacement curve and its timing is around 110 ms after impact, later than that of the relative acceleration. Figure 12 plots time history curves of NIC and JCS. NIC was calculated from the relative acceleration and velocity between the upper and lower ends of the cervical spine as described above. The JCS values were obtained from all the capsule elements in the cervical joints. The highest value was regarded as the representative JCS for evaluation. A comparison of Figure 11 and 12 finds that the time history curve of NIC is quite similar to that of the relative acceleration curve, and that JCS has its maximum peak at the same timing of the relative displacement peak.

Results of Seat Design Study

In both studies on seat design, the nodal output data and element output data were obtained first as in the rear impact simulation conducted previously. NIC, JCS, HRCT and NLA were obtained in each case. Table 2 summarizes the calculated indicator values for the thirteen cases conducted in the first study.

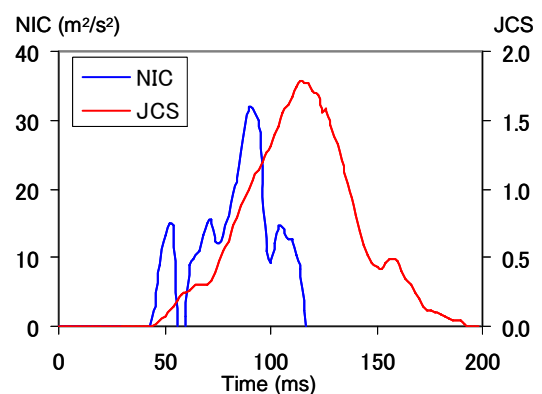


Figure 12. Time History Curves of NIC and JCS.

The calculated NIC values ranged from 10.91 to 42.38, JCS ranged from 0.492 to 1.140, HRCT was found between 49.7 and 79.4, and NLA was obtained from 5.48 to 13.61. The lowest NIC value of 10.91 was obtained in the case where the head restraint was located at the front-most and highest position. The same case showed the smallest number for HRCT. The smallest JCS value of 0.492 was found in the case where the thickness of the upper-end seat-back frame was increased. The same case showed the smallest NLA among the cases.

Figure 13 plots the trends of NIC and JCS changes for each design parameter. When the stiffness of the head restraint was changed, neither NIC nor JCS showed big changes. Both values decreased when the head restraint was moved forward. The magnitude of changes was relatively smaller when the vertical position of the head restraint was 35 mm. The stiffness of the reclining joint in rotation and in the vertical direction only affected NIC, while the thickness of the upper-end seat-back frame had a great influence on JCS but not on NIC.

Figure 14 shows the relationship among the indicators. The correlations between NIC and HRCT, NIC and NLA, JCS and HRCT, JCS and NLA were plotted. The values were obtained from the thirteen cases. The first plot suggests that NIC strongly correlates with HRCT, although its correlation is not linear. No prominent correlations were found in the next two plots, between NIC and NLA, and between JCS and HRCT. There is a strong correlation between JCS and NLA as shown in the last plot. The R^2 value was 0.917 for this case.

Table 3 shows the result of the other seat design

study on the different seat configurations. The data for Seat B is the same as that of Case 1 in Table 1. Compared to this case, Seat A showed relatively higher NIC (35.80 > 18.25), larger JCS (1.790 > 1.010), longer HRCT (70.6 > 65.8), and greater NLA (26.80 > 12.36), while Seat C gave relatively higher NIC (21.79 > 18.25), but smaller JCS (0.616 < 1.010), shorter HRCT (58.6 < 65.8), and less NLA (6.49 < 12.36).

DISCUSSION

Comparing the time history curves of acceleration and the contact forces plotted in Figure 9 and 10, it was noted that the timings of acceleration rises and their maximum peaks basically correlate with those in the contact forces. For example, both the pelvis acceleration and contact force start around 30 ms and their maximum peaks appear around 75 ms. It is considered that this acceleration is a result of motion change induced by the external force. Assuming that the motion can be simply described using Newton's laws, the amplitude of acceleration depends on the magnitude of the applied force and the mass of the part. The relatively high pelvis acceleration is mostly generated by the large contact force. The deformation of the seat-back frame generally occurs around the reclining joint. When loading the seat-back frame, the moment arm becomes shorter as the loading point is closer to the joint center. The seat-back frame generally has relatively wider sectional geometry in its lower-end part. Even if the seat-back pushes the occupant body in a horizontal direction, the contact force tends to be larger in the

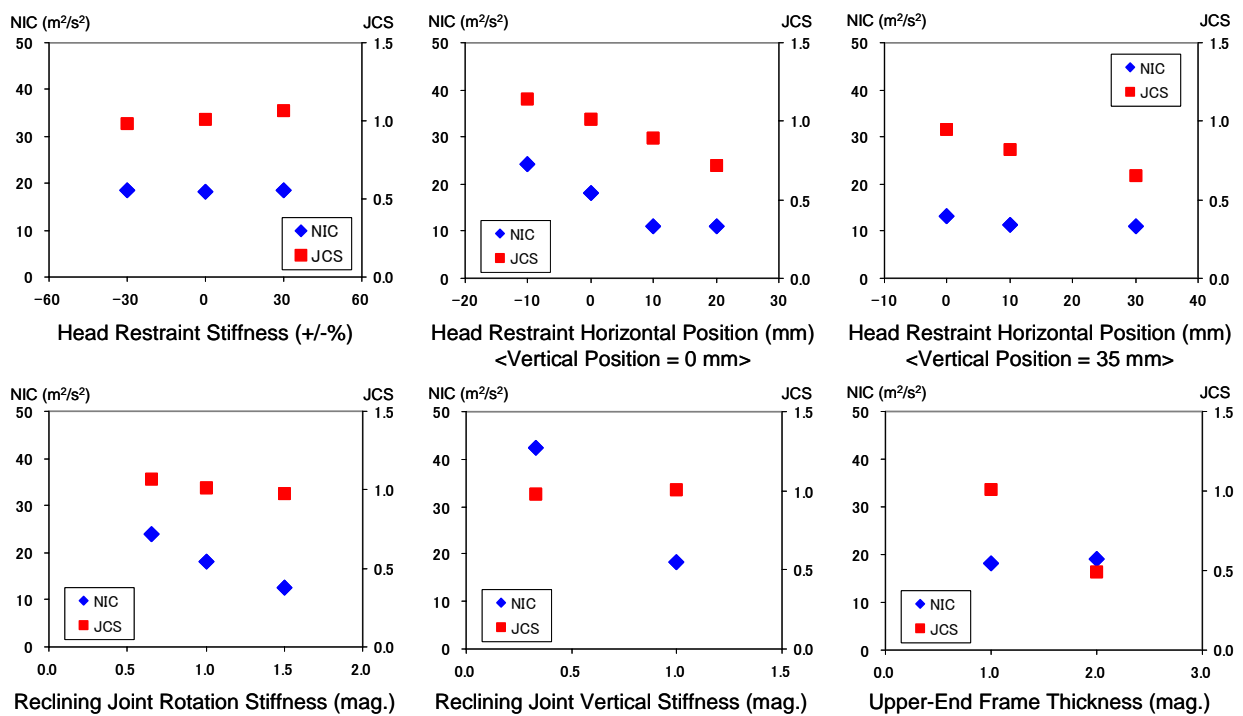


Figure 13. Correlation among Indicators.

pelvis area compared to that in the upper area. The effective mass of the pelvis is higher than the thorax or the head. Despite the relatively heavier weight, however, the pelvis can be accelerated strongly because of the greater magnitude of the contact force. Conversely, the higher acceleration of the head comes from its light mass. However, the contact force between the head and the head restraint is very small. Less stiffness in the upper part of the seat-back frame may be a reason for the small magnitude of contact force. The other possible reason is that the head restraint moves away from the occiput as the seat-back deforms backward. Although the magnitude of contact force is smaller, the head was accelerated greatly because of its smaller mass, which is around 4 kg. Unlike the pelvis and the head, the thorax acceleration has two peaks. A more complicated mechanism is assumed to explain this. Actually, the timings of the acceleration peaks do not necessarily correspond to those of the contact forces. It should be noted that T1 does not directly contact the seat-back, but there is some gap between them. The T1 acceleration is generated both by the force to the torso and by that to the head. The peaks in T1 acceleration may come from such a combination of forces. The first acceleration peak appears between the peaks of the pelvis force and the thorax force, while the second peak is in between the peaks of the thorax force and the head force. The results suggest that the acceleration pulse is greatly affected by interaction between the occupant's body and the seat. The rising timings correspond to the beginning of motion while backward motion rebounds at the timing of the maximum peak. The initial peak in relative acceleration shown in Figure 11 indicates the difference between the timing of the starting motions of the head and the torso. The head stays at the initial position for a while due to inertia while the torso is pushed forward by the seat-back. After the occiput contacts the head restraint, the contact force pushes the head forward, in the same direction as the torso. The relative motion becomes smaller after the head restraint contact. In this case, however, the head restraint moves away from the occiput due to the seat-back deformation. The relative acceleration rises again until the head is supported firmly. Anyway, the relative acceleration indicates the relative motion between the head and the torso in terms of the timing of motion change. The maximum peak was observed around 90 ms after impact in this case. On the other hand, the relative displacement has its peak around 110 ms, which is later than that of the relative acceleration peak. It is considered that the relative displacement correlates more with the seat deformation. As observed in Figure 10, the timing of the maximum contact force at the seat-back is around 95 ms, while the contact force at the head restraint reaches its peak around 125 ms. Considering the fact that the seat deformation is

caused by the contact force from the occupant, the head restraint starts deforming later than the seat-back and the maximum deformation also appears later. This is rational based on the nature of seat deformation mentioned above. The maximum relative displacement between the head and T1 is actually the difference between their positions, while the relative acceleration indicates only the difference in the timings of the starting motions. In other words, the relative displacement is the resultant difference in position induced by the contact force, but is more affected by the seat deformation. It appears that the surface geometry of the deformed seat determines the position of the occiput and the torso back. The difference in position between the head and T1 represents a neck extension when the head is relatively on the posterior side compared to T1. The timing of the NIC peak observed in Figure 12 is almost the same as that of the relative acceleration peak between the head and T1. Based on the NIC formulation ⁽¹⁾, it is obvious that the NIC value is highly affected by the acceleration term.

$$NIC=0.2*(ATI-AHead)+(VTI-VHead)^2 \quad (1).$$

where *AHead* and *ATI* are the accelerations measured at the head and T1 respectively, and *VHead* and *VTI* are the velocities at the head and T1. The timing of JCS is, on the other hand, close to that of the maximum relative displacement. This is again rational considering the fact that the relative displacement between the head and T1 indicates a neck extension. Any neck motions accompany deformation in the cervical joints. The deformation can stretch or shear the joints, causing strain in the joint capsules. Therefore, JCS is an inevitable result of cervical joint motion. This is why the timing of peak JCS is close to that of the maximum relative displacement. The timings are not exactly the same because the difference in position between the head and T1 is a summation of the joint motions from OC-C1 to C7-T1.

These findings explain possible reasons for the correlation among the indicators, obtained from the parametric study shown in Figure 14. It has already been described that the relative acceleration between the head and T1 has its peak at the timing of head restraint contact, and that NIC is mostly given by the relative acceleration. It was also explained that JCS originates from the joint deformation attributed to neck extension, and NLA actually means the magnitude of neck extension. Therefore, the correlation between NIC and HRCT, and that among JCS and NLA are reasonable considering the findings from the results obtained from the study. It should be noted, however, that HRCT is a major factor affecting NIC but not the sole element. The contact timing determines the duration in which the relative acceleration is taken into account. The

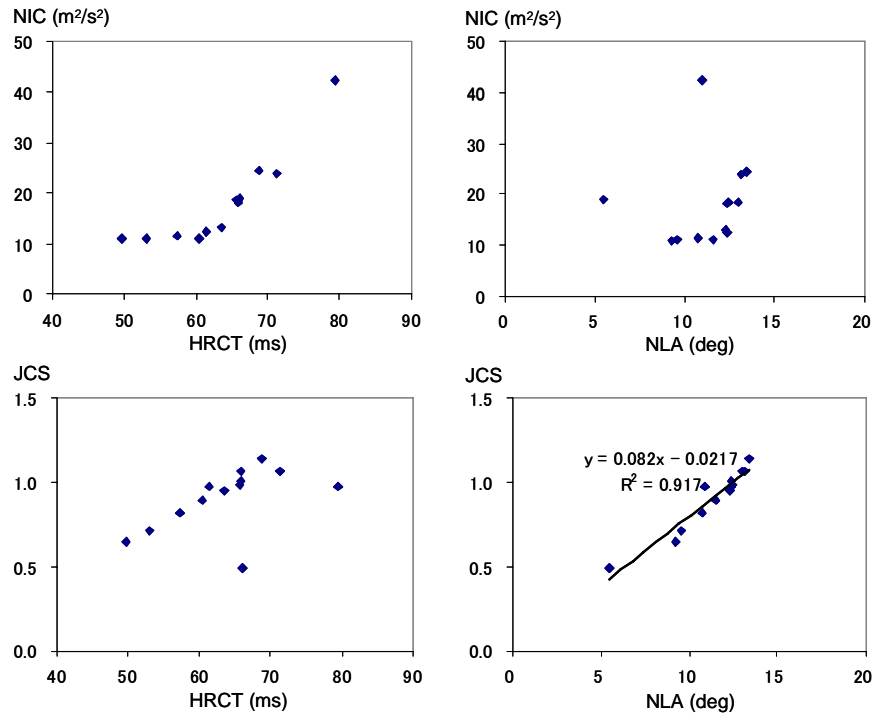


Figure 14. Correlation among Indicators.

maximum amplitude of relative acceleration in that duration actually gives the NIC value. Because the head acceleration is quite small before contacting the head restraint, the amplitude mostly comes from the T1 acceleration level. It should be remembered that the first study was conducted on a single seat configuration, which means that the resultant T1 acceleration curves are similar to one another among the cases. It is a natural result that the difference in NIC is mostly given by HRCT. Figure 15 explains the mechanism. The time history curves of the T1 acceleration, the head acceleration and NIC are plotted for Cases 1, 8 and 9. The difference in seat configuration among the cases is the location of the head restraint. The head restraint was located at the original position in Case 1. It was 10 mm ahead of the original position in Case 9 and 10 mm rearward in Case 8. The T1 acceleration pulses are close to one another while the timings of the rises in head acceleration are different between the cases. The timings of the head acceleration rises correspond to HRCT in each case. It is clear that NIC is mostly given by the T1 acceleration level at the contact time. It should be also noted that the T1 acceleration pulse in this seat has a flat level from 45 to 60 ms. This is the reason why NIC does not decrease any more when HRCT becomes shorter than 60 ms. The nonlinear correlation between NIC and HRCT shown in Figure 14 comes from the plateau in the T1 acceleration curve. If the seat configurations are different among the cases to be compared, however, the T1 accelerations may be different. This may show that HRCT does not directly indicate which seat gives a lower or higher NIC value.

Looking at the results of the other study on the different seat configurations as summarized in Table 2, it is noted that Seat C shows a higher NIC value than Seat B despite a shorter HRCT. This is possibly because the T1 accelerations are different between the two cases. Figure 16 shows the time history curves of T1 acceleration for the three cases. A comparison shows a relatively lower T1 acceleration

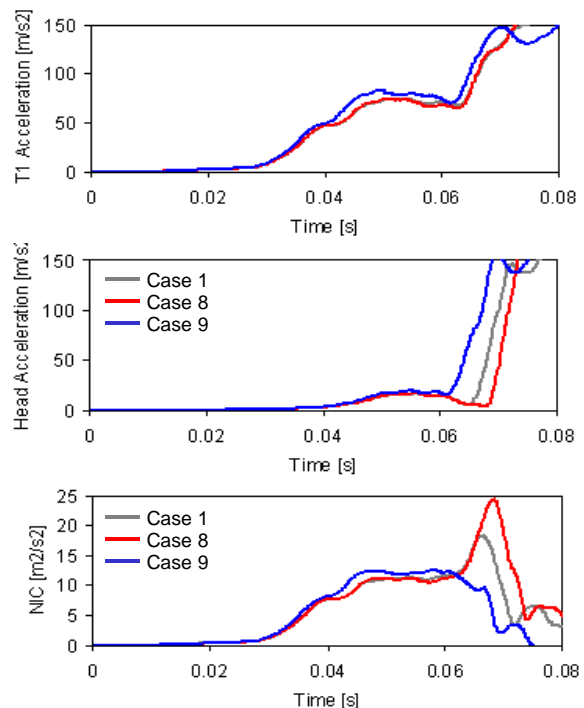


Figure 15. Time History Curves of NIC and JCS.

in Seat A. The low acceleration comes from the lower stiffness in the reclining joint. A larger deformation of the seat-back frame reduces the amplitude of T1 acceleration. The amplitude of T1 acceleration in Seat C is slightly higher but close to that in Seat B, but the profile of the acceleration pulse is different. Figure 17 inserts the NIC and JCS values into the plots showing the correlation among the indicators. Only the plots of NIC-HRCT and JCS-NLA were examined as these combinations showed strong correlations. It is found that the inserted NIC value does not follow the correlation with HRCT that was derived from the first study on a single seat configuration. This is because the three seats had different T1 acceleration pulses as shown in Figure 16. The result suggests that the validity of HRCT in terms of whiplash injury assessment is limited to a comparison among design changes on a single seat configuration. On the other hand, the inserted JCS values were found to be almost on the correlation line between JCS and NLA. This suggests that NLA can predict increase or decrease of JCS when the seat design is changed or even among different seat configurations. JCS can be calculated in the THUMS occupant model used in this study but not measured on a crash dummy. NLA can be obtained even from a dummy if the kinematics of the head and the torso are monitored. Assuming that JCS is a valid indicator to assess whiplash injury risk, NLA can be an alternative indicator for injury assessment with a dummy. A possible technical issue is that the accuracy in measuring rotational angle is less reliable compared to that when measuring acceleration or force. An alternative measurement could be neck moment assuming a linear relationship between the moment and the rotational angle. It should be re-stated that the joint capsule model used in this study tends to overestimate the strain level. A future study will focus on improving the joint capsule model to predict the strain level more accurately.

CONCLUSIONS

Rear impact simulations were conducted using a human body FE model, THUMS Version 1.61, representing a male occupant with an average body size. The model included the cervical joint capsules, which are considered as a potential site of neck pain, to calculate the strain level due to neck deformation. The model was then validated against PMHS test data obtained from the literature. Although the calculated displacement and rotation data were found almost within the test corridors, the model tended to overestimate the strain level. Only relative comparisons were therefore adopted in the following studies.

Prototype seat models were also prepared to simulate actual rear impact conditions. Their mechanical

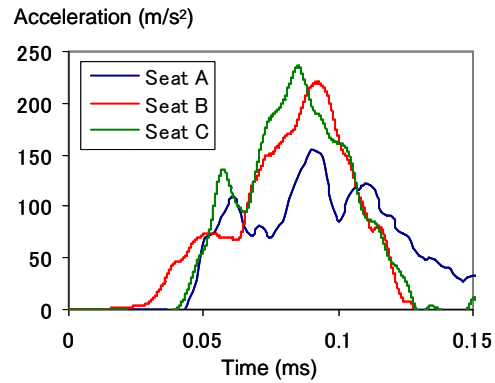


Figure 16. Comparison of T1 Accelerations.

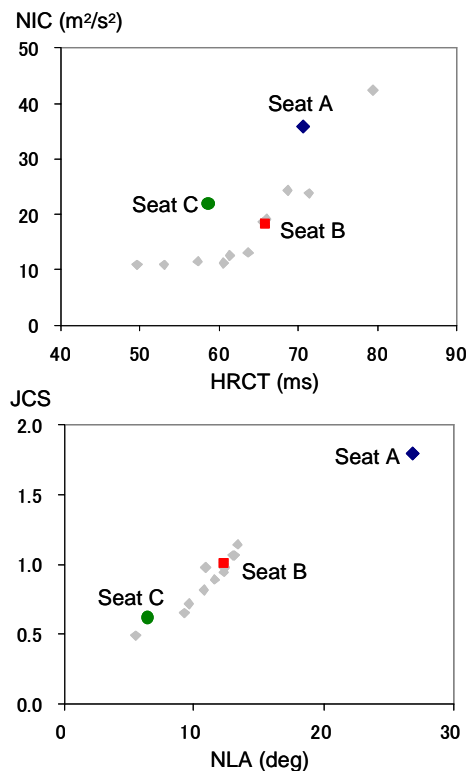


Figure 17. Correlations among Indicators in Different Seat Configurations.

responses were validated against loading test data. A rear impact simulation was conducted at a delta-V of 25 km/h. The head and neck motions and responses were analyzed in correlation with timings of rises and peaks in acceleration and force. NIC was calculated from the nodal acceleration and velocity output from the model, and JCS was obtained directly from the elements representing the capsule tissues. The results suggested that NIC indicates the difference in motion between the head and the torso while JCS indicates the difference in their positions. A parametric study was conducted on thirteen cases where major seat design factors were changed on a single seat configuration. It was shown from the results that the stiffness of the reclining joint affects the resultant NIC values while JCS is more

influenced by the thickness of the upper-end of the seat-back frame. The forward position of the head restraint was effective for both indicators. As for the relationship among the indicators, relatively strong correlations were found between NIC and HRCT, and JCS and NLA. It was explained that NIC was mostly given by the T1 acceleration level at the timing of head to head restraint contact. HRCT is, therefore, thought to be useful for comparison. The second study focused on the difference in overall seat design, that is relatively larger design changes compared to minor changes in characteristics. Three prototype seat models with different configurations were used for the study. The results showed a case showing higher NIC with shorter HRCT. The results suggested that HRCT could be useful to compare seats with design changes and the same configuration, but not necessarily for injury assessment among different seat configurations. Introducing the results of the second study into that of the first one, NLA is thought to be an alternative indicator to help assess whiplash injury risk instead of JCS in dummy tests.

ACKNOWLEDGMENTS

THUMS has been developed in collaboration with the Toyota Central Research and Development Laboratory. The authors would like to thank Toyota Technical Development Corporation for its assistance with the modeling and simulation work.

REFERENCES

- [1] Japanese National Police Agency. 2004. "Traffic Green Paper 2003" (in Japanese). 1-23.
- [2] Deng, B., P. Begeman, K. Yang, S. Tashman and A. King. 2000. "Kinematics of Human Cadaver Cervical Spine During Low Speed Rear-End Impacts." *Stapp Car Crash Journal* 44: 171-188.
- [3] Ono, K. and K. Kaneoka. 1997. "Motion Analysis of Human Cervical Vertebrae During Low Speed Rear Impacts by the Simulated Sled." *Proc. International Conference on the Biomechanics of Impacts*. 223-237.
- [4] Svensson, Y., B. Aldman, P. Lövsund et al. 1993. "Pressure Effects in the Spinal Canal During Whiplash Extension Motion: A Possible Cause of Injury to the Cervical Spinal Ganglia." *Proc. International Conference on the Biomechanics of Impacts*. 189-200.
- [5] Böstrom, O., M. Svensson, B. Aldman, H. Hansson, Y. Haland, P. Lovsund, T. Seeman, A. Suneson, A. Saljo and T. Ortengen. 1996. "A New Neck Injury Criterion Candidate Based on Injury Findings in the Cervical Spinala Ganglia after Experimental Neck Extension Trauma." *Proc. International Conference on the Biomechanics of Impacts*. 123-136.
- [6] Winkelstein, B., R. Nightingale, W. Richardson and B. Myers. 1999. "Cervical Facet Joint Mechanics: Its Application to Whiplash Injury." *Proc. 43rd Stapp Car Crash Conference*. 243-265.
- [7] Sundararajan, S., P. Prasad, C. Demetropoulos, S. Tashman, P. Begeman, K. Yang and A. King. 2004. "Effect of Head-Neck Position on Cervical Facet Stretch of Post Mortem Human Subjects during Low Speed Rear End Impacts." *Stapp Car Crash Journal* 48: 1-42.
- [8] Lu, Y., C. Chen, S. Kallakuri, A. Patwardhan and J. Cavanaugh. 2005. "Neural Response of Cervical Facet Joint Capsule to Stretch: A Study of Whiplash Pain Mechanism." *Stapp Car Crash Journal* 49: 49-66.
- [9] Yamada, H. 1970. "Strength of Biological Materials." Evans, F. G. (Ed). Williams & Wilkins Company, Baltimore.
- [10] Yoganandan, N., A. Pinter, S. Kumaresan and A. Elhagediab. 1998. "Biomechanical Assessment of Human Cervical Spine Ligaments." *42nd Stapp Car Crash Conference*.
- [11] Hasegawa, J. 2004. "A Study of Neck Soft Tissue Injury Mechanisms During Whiplash Using Human FE Model." *Proc. International Conference on the Biomechanics of Impacts*. 321-322.
- [12] Iwamoto, M., Y. Kisanuki, I. Watanabe, K. Furusu, K. Miki and J. Hasegawa. 2002. "Development of a Finite Element Model of the Total Human Model for Safety (THUMS) and Application to Injury Reconstruction." *Proc. International Conference on the Biomechanics of Impacts*. 31-42.
- [13] Kitagawa, Y., T. Yasuki and J. Hasegawa. 2006. "A Study of Cervical Spine Kinematics and Joint Capsule Strain in Rear Impacts Using a Human FE Model." *Stapp Car Crash Journal* 50: 545-566.
- [14] Siegmund, G. P., B. S. Myers, M. B. Davis, H. F. Bohnet and B. A. Winkelstein. 2000. "Human Cervical Motion Segment Flexibility and Facet Capsular Ligament Strain under Combined Posterior Shear, Extension and Axial Compression." *Stapp Car Crash Journal* 44: 159-170.

[15] Kraft, R., A. Kullugren, A. Ydenius, O. Bostrom, Y. Haland and C. Tingvall. "Rear Impact Neck Protection by Reducing Occupant Forward Acceleration – A Study of Cars on Swedish Roads Equipped with Crash Recorders and a New Anti-Whiplash Device." Proc. International Conference on the Biomechanics of Impacts. 221-231.

[16] Ministry of Land, Infrastructure and Transport. 2002. The 3rd Car Safety Symposium.

Table 1.
Simulation Matrix for Parametric Study

Case#	Head Restraint Stiffness	Head Restraint Fore-aft Position	Head Restraint Vertical Position	Reclining Joint Rotation Stiffness	Reclining Joint Vertical Stiffness	Upper-End Frame Thickness
1	±0	±0	±0	±0	±0	±0
2	-30%					
3	+30%					
4				x1.5		
5				x0.65		
6						x2.0
7					x0.33	
8		-10				
9		+10				
10		+20				
11			+35			
12		+10	+35			
13		+30	+35			

Table 2.
Summary of Results from Parametric Study

Case#	NIC (m2/s2)	JCS	HRCT	NLA (deg)
1	18.25	1.010	65.8	12.36
2	18.56	0.981	65.6	12.47
3	18.47	1.067	65.8	12.99
4	12.48	0.978	61.4	12.36
5	23.78	1.066	71.3	13.14
6	19.00	0.492	66	5.48
7	42.38	0.978	79.4	10.93
8	24.36	1.140	68.7	13.41
9	11.08	0.892	60.5	11.55
10	11.04	0.717	53.1	9.61
11	13.08	0.949	63.6	12.28
12	11.42	0.816	57.3	10.77
13	10.91	0.649	49.7	9.23

Table 3.
Comparison among Different Seat Configurations

Seat Model	NIC (m2/s2)	JCS	HRCT	NLA (deg)
Seat A	35.80	1.790	70.6	26.80
Seat B	18.25	1.010	65.8	12.36
Seat C	21.79	0.616	58.6	6.49